Title

Induction of meibocyte differentiation by three-dimensional, matrigel culture of immortalized human meibomian gland epithelial cells to form acinar organoids.

Authors

Nuwormegbe, Selikem
Park, Na-Young
Park, Hee
et al.

Publication Date

2022-10-01

DOI

10.1016/j.jtos.2022.10.004

Peer reviewed

HHS Public Access

Author manuscript

Ocul Surf. Author manuscript; available in PMC 2023 October 27.

Published in final edited form as:

Ocul Surf. 2022 October ; 26: 271–282. doi:10.1016/j.jtos.2022.10.004.

Induction of meibocyte differentiation by three-dimensional, matrigel culture of immortalized human meibomian gland epithelial cells to form acinar organoids

Selikem Nuwormegbe[b], **Na-Young Park**[b], **Hee Joo Park**[b], **Yeonwoo Jin**[a], **Sun Woong Kim**[a,b,**,1], **James V. Jester**[c,*,1]

[a]Department of Ophthalmology, Yonsei University, Wonju College of Medicine, Wonju, Ilsan-ro, Gangwon-do, 26426, Republic of Korea

[b]Research Institute of Metabolism and Inflammation, Yonsei University, Wonju College of Medicine, Wonju, Ilsan-ro, Gangwon-do, 26426, Republic of Korea

[c]Gavin Herbert Eye Institute, University of California, Irvine, Irvine, CA, USA

Abstract

Purpose: Recent studies have shown that two-dimensional (2D) culture of primary rabbit and immortalized human meibomian gland epithelial cells (iHMGEC) do not recapitulate normal meibocyte differentiation and fail to express critical enzymes necessary for synthesis of meibum lipids. The purpose of this study was to test the hypothesis that 3D-spheroid culture of iHMGEC can facilitate meibocyte differentiation and induce the expression of acyl-CoA wax-alcohol acyltransferase 2 (AWAT2), shown to be required for synthesis of meibum wax esters.

Methods: iHMGEC were suspended in matrigel/basement membrane matrix and grown in proliferation media to form distinct cell clusters or spheroids. Cells were then treated with serum-free, differentiation media (advanced DMEM/F12) with and without FGF10 and synthetic agonists for the nuclear lipid receptor, peroxisome pro-liferator activator receptor gamma (PPARγ). Cells were then evaluated for differentiation markers using western blotting, immunocytochemistry (ICC) and real-time PCR. Control cells were grown in standard 2D culture systems.

Results: Under proliferative conditions, 3D culture induced the formation of KRT5+ spheroids that contained a Ki67+/P63+ undifferentiated, basal cell population. When spheroids were switched to differentiation media containing PPARγ agonists, two different organoid populations were detected, a $KRT6^{low}$ population that was AWAT2+/PPARγ+ and a $KRT6^{high}$ population that was AWAT2−/PPARγ−, suggesting that iHMGEC exhibit a dual differentiation potential toward either a ductal or meibocyte organoid phenotype.

**Corresponding author. Department of Ophthalmology, Yonsei University, Wonju College of Medicine, Wonju, Ilsan-ro, Gangwon-do, 26426, Republic of Korea. eyedockim@yonsei.ac.kr (S.W. Kim). *Corresponding author. 843 Health Sciences Road, University of California Irvine, Irvine, CA, 92697-4390, United States. JJester@hs.uci.edu (J.V. Jester).

[1]Both authors contributed equally.

Declaration of competing interest

The authors have no commercial interest in any concept or product discussed in this article.

Appendix A. Supplementary data

Supplementary data to this article can be found online at https://doi.org/10.1016/j.jtos.2022.10.004.

Conclusion: The 3D culturing of iHMGEC can induce the formation of both meibocyte and ductal organoids and may thus serve as a better in vitro model system for studying the regulatory mechanisms controlling meibomian gland function.

Keywords

AWAT2; dry eye; Meibocytes; Meibomian gland dysfunction; Meibum; PPAR-γ; Two dimensional culture system; Three dimensional culture system; Acinar organoids

1. Introduction

The meibomian gland (MG) is a holocrine secretory gland, similar to sebaceous glands, that is comprised of a long central duct lined with ductal epithelial cells and attached acini comprised of lipid synthesizing meibocytes [1–3]. Fully differentiated meibocytes produce and secrete a lipid-rich compound called meibum, which is largely made up of neutral/nonpolar lipids, such as wax esters (WE), cholesteryl esters (CE), triacylglycerols (TAG), (O-acyl)-ω-hydroxy fatty acids (OAHFA) and free cholesterol (Chl), and smaller amounts of polar lipids such as phospholipids (PL), free fatty acids (FFA), ceramides (Cer), and sphingomyelins (SM) [4–9]. The secreted meibum is delivered by the central duct to the eyelid margin and onto the ocular surface where it forms the tear film lipid layer (TFLL) that stabilizes the tear film and retards tear evaporation [10–12].

Meibomian gland dysfunction (MGD) is a disorder caused by functional and/or anatomical abnormalities of the MG leading to altered meibum quality and aberrant secretion [13–16]. MGD is broadly classified based on the clinical impression of the secretory state of the gland into high delivery (hypersecretion) MGD, or low delivery (hyposecretion or obstruction) MGD, for which the underlying pathogenetic mechanisms are poorly understood [13,14]. Low delivery MGD is associated with an evaporative dry eye disease (DED), which is an ocular surface disorder characterized by unstable tear film, increased tear evaporation and tear film hyperosmolarity that causes ocular surface irritation, inflammation, discomfort, fatigue and impaired vision [13–17]. MGD accounts for about two-thirds of all DED, and is a rising public health concern, especially among women and the elderly [14,16].

Current treatments for MGD and DED are lacking and/or ineffective, and it is thought that understanding the cellular and molecular mechanisms controlling meibomian gland function, progenitor cell renewal, gland keratinization, lipid/meibum synthesis and meibum secretion would help in identifying new and more effective therapies. For the most part, studies have used an immortalized human meibomian gland epithelial cell line (iHMGEC) [18] that has been noted to have many limitations, including differentiation conditions that favor a ductal keratinization pathway [19], the formation of lipid droplets in the lysosomal/degradation intracellular compartment [20], absence of the biosynthesis of WE and other major meibum lipids [21], as well as many other concerns that have been recently reviewed in depth by Phan et al. [22]. Of particular concern has been the failure to detect the expression and/or upregulation of critical enzymes known to be required for the synthesis of meibum specific lipids, particularly acyl-CoA wax-alcohol acyltransferase 2 (AWAT2).

AWAT2 is required for the synthesis of WE by the meibomian gland, and deletion of this enzyme reportedly leads to an MGD and DED phenotype in mice [23,24]. Recent studies have also shown that AWAT2 expression abruptly disappears when primary cells are placed in culture and that expression is not up-regulated when progenitor meibocytes are induced to differentiate and synthesize lipids under standard culture conditions [25].

One possible explanation for these findings is that normal meibocyte differentiation requires contextual signals that are not provided to cells attached to planar, 2 dimensional (2D) surfaces. In this regard, three-dimensional (3D)/multilayer cell culture system, which permits cell-cell and cell-matrix interactions similar to physiological conditions [22,26], may thus provide a more suitable microenvironment for the activation of such biological signals as occurs in MG acini. Indeed, 3D cultures have been studied using sebocytes which share many similarities with meibocytes [27]. The only 3D culture study using iHMGEC was published by Asano et al. [28] using hard polymer scaffolds and showed cytoplasmic lipid droplet accumulation over a longer period of time, indicating the ability of iHMGEC to differentiate in long-term 3D cultures. However, no analysis of the lipid composition or expressions of lipid synthesizing enzymes were reported.

In this study, we aimed to evaluate the 3D culture of iHMGEC using the thermo reversible protein-based, extracellular matrix (ECM), matrigel. Matrigel is a self-polymerizing, ECM based hydrogel, consisting of laminin (~90%), collagen, entactin, heparin sulfate proteoglycans, matrix metalloproteinases (MMP), and several growth factors, extracted from the basement membrane of the mouse sarcoma, Engelberth–Holm–Swarm (EHS) [29]. In previous studies using immortalized sebocytes, 3D culture in matrigel induced spheroid formation that showed mature, differentiated sebocytes with lipid droplets surrounded by undifferentiated, stem-like sebocytes [30]. We therefore hypothesized that 3D culture of iHMGEC with matrigel would induce the formation of spheroids that could differentiate toward meibocyte organoids with centrally located mature differentiated cells surrounded by basal proliferating cells, mimicking normal MG acinar structure.

2. Materials and methods

2.1. Two-dimensional cell culture

iHMGEC, a generous gift from Dr Sullivan, (Schepens Eye Research Institute, Boston, MA, USA) were used in this study. The cells were cultured until 80% confluent in a 6 well plate with proliferation media, comprised of keratinocyte serum free media (KSFM) supplemented with bovine pituitary extract (BPE) and recombinant human epidermal growth factor (EGF) (Gibco Life Technologies, Waltham, MA USA), as well as 20 ng/mL recombinant human fibroblast growth factor (FGF-10) (PeproTech, Seoul, Korea), a growth factor required for the development of meibomian and lacrimal glands [31], and 1% antibiotics/antimycotics (streptomycin, penicillin, and amphotericin B; Gibco Life Technologies). After confluency, media was changed to a differentiation media comprised of advanced Dulbecco's Modified Eagle Medium:Nutrient Mixture F-12 (DMEM/F-12) (Gibco Life Technologies) supplemented with 20 ng/mL FGF-10, 20 ng/mL EGF, (PeproTech) and 1% antibiotics/antimycotics. Various studies have shown that PPAR-γ signaling, activated by synthetic or natural ligands (i.e. essential fatty acids), is required for meibocytes

differentiation [1,32]. Therefore to initiate differentiation, cells were treated with the synthetic PPARγ ligands, rosiglitazone (Cayman Chemical, Ann Arbor, MI, USA) at 20 μM and lobeglitazone (Chong Keun Dang Pharmaceutical Corp., Seoul, South Korea) at 5 μM dissolved in dimethyl sulfoxide (Duchefa Biochemie, Haarlem, Netherlands) and incubated up to 5 days to achieve maximum lipid accumulation [33]. Vehicle treated cells were used as control. The media was renewed every 2 days. The incubation period was determined by prior cell viability experiments with trypan blue assay. Cell viability remained over 95% during proliferation and between 85% and 90% for both the control and PPARγ ligand treatment groups after 1 week differentiation.

After differentiation, the cells were detached with 0.25% trypsin (Gibco Life Technologies), transferred into 1.5 mL Eppendorf tubes and centrifuged at 1500×*g* for 5 min. The supernatant was discarded and the cells pellets retrieved for biochemical analysis. The appearance of the cells was documented before and after differentiation using the Invitrogen™ EVOS™ XL core imaging system, (Thermo Fisher Scientific, Bothell,WA, USA) at 10X magnification.

2.2. Three-dimensional cell culture

To induce spheroid formation and mimic acinar structure, we seeded iHMGEC into matrigel and cultured cells in proliferation media for up to three weeks as illustrated diagrammatically in Fig. 1. iHMGEC were suspended in KSFM at 4 °C and added to Corning® Matrigel® Growth Factor Reduced (GFR) Basement Membrane Matrix (Discovery Labware Inc., Bedford, MA) at 4 °C, to achieve a 4:1 matrigel:KSFM dilution (80% matrigel) at a final concentration of 5 x 10^4 cell/ml. Fifty micro liters (50 μL) of the cold matrigel/iHMGEC suspension (2.5 x 10^3 cells) was then pipetted into each well of a 24 well plate (Corning Incorporated, Keennebunk, ME, USA) to form a dome in the center of the wells. This number of cells avoided overcrowding so as to allow room for the formation of large and distinct spheroids.

The plate was then incubated for 30–60 min at 37 °C in a humidified 5% CO_2 incubator to polymerize the matrigel. The KSFM proliferating media was then added to each well and incubated at 37 °C in a humidified 5% CO_2 incubator to allow the cells to grow and proliferate. iHMGEC spheroids began to form after 3 days of incubation and became more obvious after 1 week of incubation. The spheroids were cultured for 2 more weeks, making a total of 3 weeks of the proliferation with media changes every two days, within which time most spheroids grew in size to greater than 100 μm diameter, in close proximity to the human MG acini diameter size of 150 μm–200 μm [15]. After three weeks, the proliferation media was changed to differentiation media supplemented with FGF10 and EGF with and without 20 μM rosiglitazone or 5 μM lobeglitazone. To confirm PPARγ signaling effects, cultures were also treated with 5 μM GW9662 (Tocris Bioscience, Bristol, UK), a synthetic PPARγ inhibitor. Vehicle treated cells/spheroids were used as control. Cells were then incubated for one week with media changed every 2 days. The incubation period was determined prior by cell viability experiments with trypan blue assay. Cell viability was over 90% during proliferation and averaged 76.5% for the control groups and 69% for the PPARγ ligand treatment groups after 1 week differentiation. Decreased viability following

differentiation was most likely due to holocrine secretion and cell death by the differentiated cells.

After one week differentiation, the media was removed and 200 μL of cell recovery solution (Discovery Labware Inc.) was added to each well. The plate was incubated at 4 °C for about 2–3 h to completely dissolve the matrigel. The solution containing the spheroids was then transferred into 1.5 mL Eppendorf tubes and then centrifuged at 1500×*g* for 5 min, the supernatant discarded, and the cells/spheroids pellets retrieved for biochemical analysis. Spheroid appearance was documented during the course of the culture period using an EVOS™ XL core microscope at 10X magnification.

2.3. Real time PCR

To evaluate iHMGEC proliferation and differentiation in our 3D culture system compared to the 2D culture system, we analyzed the transcription of the progenitor/stem cell marker, leucine-rich repeats and immunoglobulin-like domains 1 (LRIG1), a type 1 transmembrane protein found to be stimulated and accumulated in proliferating iHMGEC [34,35], and the meibocytes differentiation marker AWAT2 [36]. PPAR-γ signal activation was also confirmed by perilipin 2 (PLIN2) transcription, a lipid droplet-associated protein [37]. Total RNA was extracted with an extraction kit (Qiagen, Hilden, Germany) following the manufacturer's protocol. The quality and quantity of the RNA extracts were assessed with NanoDrop One spectrophotometer (Thermo Fisher Scientific). RNA quality (A260/A280 ratio) ≥ 1.8 was used for further processes. LaboPass™ cDNA synthesis kit (Cosmo Genetech, Seoul, Korea) was used to synthesize cDNA according to the manufacturer's protocol. RT-qPCR was done with primer pairs of target genes in a 10 μL reaction mixture with SYBR green PCR mix (Applied Biosystems, Life Technologies, Foster City, CA, USA). The experiments were done in triplicates. Relative quantitation was performed using the comparative Ct method using GAPDH as the normalizing housekeeper gene. The list of the primer pair sequences used are provided in Supplemental Table 1.

2.4. Western blot

Western blotting was performed to determine the expression of AWAT2 protein to ascertain the presence or absence of translation signals, since 3D cultures allow cellular communications which are not present in 2D cultures [22]. Total protein was extracted with radio-immunoprecipitation assay (RIPA) buffer (Thermo Fisher Scientific) with phosphatase and protease inhibitors (Roche Diagnostic GmbH, Mannhiem, Germany). After protein quantification with bradford assay reagent (Bio-Rad Laboratories, Inc. Hercules, CA, USA), 50 μg of the cell extract was run on 10% sodium dodecyl sulfate polyacrylamide gels and then transferred onto polyvinylidene fluoride membranes (Millipore, Italy). The membranes were blocked with 5% skimmed milk solution prepared with 1X Tris-buffered saline with 0.1% Tween® 20 detergent (1X TBST) for 2 h on a shaker at room temperature, washed and incubated with primary antibodies (list provided in Supplemental Table 2) overnight on a shaker at 4 °C. Membranes were washed (3 × 5 min) with 1X TBST, followed by incubation with horseradish peroxidase-conjugated secondary antibody for 2 h at room temperature. The membranes were finally washed (3 × 5 min) with 1X TBST and the blots detected with Pierce™ enhanced chemiluminescence western blotting substrate (Thermo Fisher Scientific,

Rockford, IL USA). The immunostained band images were captured with Image Lab™ software version 6.0.1 (Bio-Rad Laboratories Inc.). The relative quantization of the target protein AWAT2 was done after normalization to the house-keeping protein beta-actin in same blots using the Lab™ software version 6.0.1 image analysis tool. The experiments were done in triplicates.

2.5. Immunofluorescence staining

Immunofluorescence staining analyses were performed to assess the expression and localization of various proteins. The spheroids were stained with the proliferation marker, Ki67, the basal epithelial progenitor cell marker, ΔNp63, and the basal epithelial cell marker, cytokeratin 5 (KRT5), to assess the presence of progenitor/proliferating basal cells under the different culture conditions. Staining for the ductal epithelial cell marker, cytokeratin 6 (KRT6), and the meibocyte marker, PPARγ, were used to characterize the spheroids. The expression and localization of differentiated and undifferentiated cells in the spheroids was evaluated by AWAT2 and LRIG1 respectively.

Spheroids embedded in the matrigel were fixed with 4% paraformaldehyde overnight at 4 °C. The spheroids were then cryoprotected by directly perfusing with 30% sucrose solution overnight at 4 °C after which they were embedded in optimal cutting temperature (OCT) compound (Sakura Finetek, Torrance, CA, USA) and quickly frozen. Ten micrometer (10 μm) thick sections were cut on a freezing microtome and mounted on poly-L-lysine coated slides (Fisherbrand, Pittsburgh, PA, USA). Sections were washed with phosphate buffered saline (PBS-T, 3 × 5 min), permeabilized with 0.1% Triton X-100 and then incubated in protein blocking solution (5% BSA) in PBS-T for 1 h at room temperature. After protein blocking, the slides were incubated with primary antibodies overnight at 4 °C. The slides were washed with PBS-T (3 × 15 min) and then incubated with Alexa Fluor 488 or Alexa Fluor 594 conjugated secondary antibodies (Life Technologies Corporation, Eugene, OR, USA) in the dark for 2 h at room temperature. The slides were finally washed (3 × 15 min) in 1X PBS and dried. The nuclei were stained with 4′,6-diamidino-2-phenylindole (DAPI) in mounting solution (ProLong™ Gold Antifade Mountant, Thermo Fisher Scientific) and cover slipped. Cells incubated with PBS and secondary antibodies without prior primary antibody treatments were used as negative controls. The list of primary antibodies used is provided in Supplemental Table 2.

For neutral lipid staining, sections of spheroids on poly-L-lysine coated slides were prepared as previously stated [33]. The slides were then washed with 1X PBS and incubated in HCS LipidTOX™ green neutral lipid stain (Thermo Fisher Scientific) at 1:1000 dilution for 30 min in the dark at room temperature. The slides were finally washed with PBS, mounted with DAPI mounting solution and cover slipped. The fluorescence images were captured with the Olympus BX51 fluorescence microscope (Olympus, Tokyo, Japan) using the fluorescein isothiocyanate (FITC), rhodamine and DAPI channels at 20X magnification.

To analyze differences in LRIG1 and AWAT2 immunostaining between spheroids, the average fluorescence intensity per spheroid area was calculate and used for statistical comparisons between different treatment groups. For Ki67, ΔNp63, and KRT5, the percentage of positive cells was calculated by dividing the number of positive cell by

the total number of cells. To calculate the lipid content per cell in each image, the thresholded lipid pixel area was divided by the total number of cells in each image. At least 20 spheroids of diameters 100 μm and above were analyzed per treatment group. All analyses for 3D spheroids are semi-quantitative since randomly cut sections were obtained as representative of the spheroids. Images were analyzed with Image J [https://imagej.nih.gov/ij/download.html]. All experiments were done in triplicates.

2.6. Statistical analysis

All numeric data were reported as mean ± standard error. Differences in mRNA and protein expression between different groups were assessed by one-way analysis of variance and Tukey's multiple comparisons test in both cultures using GraphPad Prism 5.0 software (GraphPad Software, USA). All experiments were repeated at least 3 times and a P value of <0.05 was considered statistically significant.

3. Results

3.1. The 3D cell culture induced formation of iHMGEC spheroids

As shown in Fig. 2A, iHMGEC cultured on planar surfaces in proliferation media alone showed a uniform rounded, epithelioid morphology with no clustering of cells throughout the culture dish. When iHMGEC were grown to near confluence (80%) and then switched to differentiation media, cells became clustered together and assumed a flattened, elongated morphology that was distinct from the epithelioid cells grown in low calcium proliferation media.

When iHMGEC cells were grown in 3D matrigel, cells formed loosely packed spheroids averaging 23.5 μm ± 0.77 in diameter by 1 week (Fig. 2B). Spheroid diameters increased significantly over time, averaging 46 μm ± 1.73 and 121 μm ± 4.20 by two and three weeks, respectively ($P < 0.001$). When the media was switched to differentiation media for one week, no significant change in spheroid size was detected, averaging 148 μm ± 3.73 (Fig. 2B), however, spheroids appeared dark by transmitted light, most likely due to the accumulation of light scattering lipid droplets as seen in normal meibomian glands [38].

3.2. Effect of FGF10 and PPAR-γ signaling on 3D cultured iHMGEC

When 3D cultured spheroids grown in proliferation media were stained with antibodies to the Ki67 (Fig. 3A), or the basal epithelial progenitor cell marker ΔNp63 (Fig. 4A), both Ki67 and ΔNp63 were detected in basal cells, averaging 27.75% ± 2.01 $Ki67^+$ (Figs. 3E) and 48.53% ± 3.03 $\Delta Np63^+$ (Fig. 4E). When spheroids were switched to DMEM/F12 media containing FGF10 there was no significant decrease in either cell proliferation, averaging 24.47% ± 1.83 $Ki67^+$ (Fig. 3, B and E) or number of progenitor cells, averaging 33.39% ± 5.90 $\Delta Np63^+$ (Fig. 4, B and E). However, when rosiglitazone was added to the culture media without the addition of FGF10, there was a significant decrease in the number of $Ki67^+$ and $\Delta Np63^+$ cells ($P < 0.001$; Fig. 3, C and E and $P < 0.001$; Fig. 4, C and E, respectively), averaging 3.17% ± 1.08 Ki67+ and 3.16% ± 1.52 ΔNp63+ cells. In contrast, maintaining spheroids in FGF10 containing media in the presence of rosiglitazone maintained significantly higher levels of cell proliferation averaging 10.77% ±

0.48 $Ki67^+$ cells (Fig. 3D and E), but still significantly lower ($P < 0.01$) than cells grown in the absence of rosiglitazone. Similarly, the numbers of progenitor cells in the basal cell layer was significantly higher with the addition of FGF10 with rosiglitazone averaging 24.78% ± 3.51 ΔNp63+ (Fig. 4D and E), which was not significantly different from that of spheroids cultured in with FGF10 alone. As shown in Fig. 5, iHMGEC differentiated with FGF10 alone maintained KRT5 expression and showed no lipid droplet accumulation (Fig. 5A and D), while spheroids differentiated with rosiglitazone with FGF10 (Fig. 5B) or rosiglitazone (Fig. 5C) both showed significantly reduced KRT5 staining limited to the basal cell compartment (Fig. 5D), and significantly increased lipid accumulation (Fig. 5E).

3.3. The 3D culture system promotes expression of meibocytes differentiation markers

We next evaluated the effect of 2D and 3D culture on expression of meibocyte differentiation markers by treating spheroids with synthetic PPARγ agonists, rosiglitazone (20 μM) and lobeglitazone (5 μM) (Fig. 6). Real-time PCR showed that activation of the PPAR-γ pathway in both 3D and 2D culture systems significantly increased PLIN2 and significantly decreased LRIG1 mRNA transcription as shown in Fig. 6A, consistent with early meibocyte differentiation and lipid synthesis (Fig. 5B and C). By contrast, expression of AWAT2, the critical enzyme required for synthesis of WE and the highest lipid enzyme expressed in the meibomian gland, was only detected in 3D spheroid cultures treated with either rosiglitazone or lobeglitazone (Fig. 6B) and not in 2D cultured cells. Interestingly, expression of AWAT2 in spheroids was localized to the suprabasal compartment similar to that detected in intact meibomian glands, and was associated with the loss of LRIG1 staining (Fig. 6C).

3.4. AWAT2 expression is modulated by PPARγ activation in spheroid culture

To determine if PPARγ signaling modulates AWAT2 synthesis, we pre-treated the cells with 5 μM of the PPARγ synthetic inhibitor GW9662 for 5 h before PPAR-γ ligand treatment. Our results showed a significant attenuation of AWAT2 protein synthesis with PPAR-γ signal inhibition (Fig. 7) while groups without the PPAR-γ signal inhibition maintained AWAT2 protein expression.

3.5. Progenitor cell derivation of iHMGEC spheroids

Previous studies have suggested that there are two separate progenitor cell populations in the meibomian gland that are KRT6+/PPARγ− or KRT6−/PPARγ+ and give rise to the ductal epithelium or the acinar meibocytes, respectively [39]. To explore the presence of these progenitor cell populations in the immortalized iHMGEC cell line, spheroids were characterized for presence of KRT6/PPARγ/AWAT2. When spheroids were grown in differentiation media without rosiglitazone, two general types of spheroids were detected as shown in Fig. 8A, a $KRT6^{low}$/AWAT2− and $KRT6^{high}$/AWAT2− expressing spheroids. However, when rosiglitazone was added to the differentiation media (Fig. 8B), $KRT6^{low}$ spheroids showed staining for both AWAT2 and PPARγ, while $KRT6^{high}$ spheroids showed no staining for AWAT2 and PPARγ. The percentage of KRT6+ cells were however highly variable in both the $KRT6^{low}$ and $KRT6^{high}$ spheroids.

4. Discussion

This report establishes, for the first time, that 3D matrigel culture of iHMGEC induces the formation of acinar-like spheroids that, when exposed to PPARγ agonists, induces the expression of the critical lipid synthesizing enzyme, AWAT2, that is required for the synthesis of WE, a principal component of meibum [23]. 3D matrigel culture also supported the apparent differentiation on iHMGEC into two different types of spheroids, a $KRT6^{low}$/AWAT2+/PPARγ+ and a $KRT6^{high}$/AWAT2−/PPARγ−. We also confirm findings of our earlier study showing that iHMGEC cultured on planar substrates only express extremely low levels of AWAT2 RNA that are not modulated by standard differentiation conditions [25]. These findings have important implications regarding our understanding of iHMGEC differentiation and their value to elucidating the cellular and molecular mechanisms regulating meibomian gland function.

First, 3D matrigel culture of iHMGEC appears to provide critical signals required for meibocyte differentiation that is not present in standard 2D culture. It may also have an advantage in providing similar polarity of differentiation as in tissues. The cell to cell and cell to matrix interactions may also have provided a more suitable microenvironment for differentiation, which is not provided to cells on 2D planar surfaces. It is well known that extracellular matrices provide unique structural support and stability to cells, as well as supporting signaling dynamics that influence cell fate [40]. In this regard, 3D matrigel culture combined with the addition of FGF10 seems to provide a niche environment necessary for the proliferation and maintenance of meibomian gland basal progenitor cells as identified by the expression of Ki67, ΔNp63 and LRIG1. These cells then give rise to early differentiating cells that appear to exit the cell cycle, lose expression of progenitor cell markers, and migrate into the suprabasal compartment. Some of these cells then give rise to more fully differentiated cells that synthesize and accumulate lipids and express AWAT2. Interestingly, basal spheroid cells in matrigel culture neither accumulate lipid nor express AWAT2, and therefore appear to mimic, in part, the organoid structure of the MG acinus. However, it should be noted that the expression level of AWAT2 protein in our 3D culture was substantially lower, compared to that of mouse meibomian glands, where RNA sequencing suggests that AWAT2 is the 13th most common transcript of the 16,000+ that were identified [41]. While the expression level of AWAT2 protein in rosiglitazone treated 3D cultures was 2–3 fold higher than untreated cultures, this level of expression is also substantially below what is detected from tissue extracts. Furthermore, not all suprabasal cells appeared to express AWAT2, unlike the expression detected within intact meibomian glands [25]. Together, these findings suggest that 3D matrigel culture does not entirely recapitulate normal meibocyte differentiation, and that additional modifications may be necessary to drive complete differentiation.

In this regard we speculated that one explanation for the limited number of suprabasal cells that express AWAT2 may be due, in part, to the possibility that iHMGEC cultures contain two progenitor cell populations, one ductal and one meibocyte. To our knowledge, the isolation protocol for iHMGEC did not describe the cloning of cells after immortalization [18], and therefore iHMGEC may contain a mixed cell population. Previous studies of iHMGEC have shown the potential to differentiate into a ductal epithelial cell lineage as first

established by Hampel et al. for 2D cultures [19], and more recently by Asano et al. for 3D air-lifted cultures [28]. However, our report appears to be the first to establish that iHMGEC can differentiate to meibocytes that express the key biomarker of sebaceous/meibomian gland differentiation, i.e. AWAT2. While we have not as yet evaluated the lipidomic profile of 3D matrigel cultured iHMGEC, our findings support the hypothesis that iHMGEC can differentiate into the two key cell populations that comprise the meibomian gland, ductal epithelial and meibocytes. We would propose that it will be important to identify whether these observations are due to the presence of a mixed or bipotent progenitor cell population within iHMGEC. Of note, we observed a very high variability in the percentage of KRT6+ cells in the individual spheroids. This may be important, in that it may lead to discrepancies in AWAT2 expression levels between spheroid cultures, since levels will depend on the relative proportion of the different cell populations.

Secondly, if AWAT2 is a critical biomarker for meibocyte differentiation that can only be expressed in 3D matrigel culture, then much of the information derived from the study of iHMGEC in 2D cultures would appear to be most relevant to understanding MG ductal epithelial differentiation. While accumulation of lipid has been used as a marker for meibocyte differentiation in 2D culture models, previous studies have shown that this lipid for the most part is detected in the lysosomal compartment [20,42–44], which is generally thought to be associated with catabolic and/or autophagic processes [45]. Furthermore, the lipidome identified in these cultures is generally agreed to be not meibum-like [22]. More recently, we have shown that PPARγ agonists can induce lipid accumulation within the endoplasmic reticulum of iHMGEC [32], a similar site identified by morphologic studies of the MG [3], and that PPARγ agonists induces a more meibum-relevant lipid profile, particularly for CE [21]. However, these findings were identified in 2D culture, and whether MG ductal epithelium can synthesize lipid in response to PPARγ agonists is not known. During development, the ductal anlage shows expression of PPARγ and the appearance of lipid at post-natal day 5, during the formation of the ductal lumen [46]. Therefore, it is possible that ductal epithelia cells can respond to PPARγ signaling and induce lipid accumulation, but whether the ductal lipidome is similar to meibum is not known and needs further study.

A final interesting finding regards the expression of progenitor and differentiation cell markers that have recently been identified in 2D culture models. In our study we used LRIG1 as a biomarker for spheroid progenitor cells based on the recent findings by Xie et al. [35], who reported the differential expression of LRIG1 and DNase2 in progenitor and differentiated iHMGEC in 2D culture. While our findings were consistent with those of Xie et al., our earlier label retaining cell studies in mice showed that 100% of acinar slow cycling/progenitor cells were SOX9+ in the meibomian gland [47]. Given that iHMGEC may differentiate into two different lineages, ductal vs meibocyte, and that 2D culture may preferentially induce ductal epithelial differentiation, more detailed study is needed to clarify which progenitor cell markers play a role in meibocyte renewal.

5. Conclusion

In summary, we introduced a novel 3D culture model that promoted iHMGEC proliferation and differentiation and may thus serve as an in vitro model for the study of meibocyte differentiation. It should be noted that the expression level of AWAT2 is still very low as compared to eyelid tissue, and that future studies need to focus on improving or modifying this system to more accurately recapitulate meibocytes differentiation in tissues. Understanding the cellular and molecular regulation of AWAT2 expression may be critical in helping to establish a culture model that could mimic physiologic differentiation.

Supplementary Material

Refer to Web version on PubMed Central for supplementary material.

Funding

This work was supported in part by NIH/NEI EY021510, an Unrestricted Grant from Research to Prevent Blindness, Inc. RPB-203478, and the Skirball program in Molecular Ophthalmology and basic science research program through the National Research Foundation of Korea (NRF) funded by the Ministry of Education, Science and Technology (2020R1I1A3073515).

References

[1]. Hwang HS, Parfitt GJ, Brown DJ, Jester JV. Meibocyte differentiation and renewal: insights into novel mechanisms of meibomian gland dysfunction (MGD). Exp Eye Res 2017;163:37–45. [PubMed: 28219733]

[2]. Nichols KK, Foulks GN, Bron AJ, Glasgow BJ, Dogru M, Tsubota K, Lemp MA, Sullivan DA. The international workshop on meibomian gland dysfunction: executive summary. Invest Ophthalmol Vis Sci 2011;52(4):1922–9. [PubMed: 21450913]

[3]. Jester JV, Nicolaides N, Smith RE. Meibomian gland studies: histologic and ultrastructural investigations. Invest Ophthalmol Vis Sci 1981;20(4):537–47. [PubMed: 7194327]

[4]. Foulks GN, Bron AJ. Meibomian gland dysfunction: a clinical scheme for description, diagnosis, classification, and grading. Ocul Surf 2003;1(3):107–26. [PubMed: 17075643]

[5]. Butovich IA, Millar TJ, Ham BM. Understanding and analyzing meibomian lipids–a review. Curr Eye Res 2008;33(5):405–20. [PubMed: 18568877]

[6]. Chun YH, Kim HR, Han K, Park Y-G, Song HJ, Na K-S. Total cholesterol and lipoprotein composition are associated with dry eye disease in Korean women. Lipids Health Dis 2013;12:84. [PubMed: 23734839]

[7]. Butovich IA, Suzuki T, Wojtowicz J, Bhat N, Yuksel S. Comprehensive profiling of Asian and Caucasian meibomian gland secretions reveals similar lipidomic signatures regardless of ethnicity. Sci Rep 2020,10:14510. [PubMed: 32883999]

[8]. Borchman D, Foulks GN, Yappert MC, Milliner SE. Differences in human meibum lipid composition with meibomian gland dysfunction using NMR and principal component analysis. Invest Ophthalmol Vis Sci 2012;53(1):337–47. [PubMed: 22131391]

[9]. McCulley JP, Shine WE. Meibomian gland function and the tear lipid layer. Ocul Surf 2003;1(3):97–106. [PubMed: 17075642]

[10]. Georgiev GA, Eftimov P, Yokoi N. Structure-function relationship of tear film lipid layer: a contemporary perspective. Exp Eye Res 2017;163:17–28. [PubMed: 28950936]

[11]. Sledge SM, Khimji H, Borchman D, Oliver AL, Michael H, Dennis EK, Gerlach D, Bhola R, Stephen E. Evaporation and hydrocarbon chain conformation of surface lipid films. Ocul Surf 2016;14:447–59. [PubMed: 27395776]

[12]. Bron AJ, Tiffany JM. The meibomian glands and tear film lipids: structure, function and control. Adv Exp Med Biol 1998;438:281–95. [PubMed: 9634898]

[13]. Chhadva P, Goldhardt R, Galor A. Meibomian gland disease: the role of gland dysfunction in dry eye disease. Ophthalmology 2017;124(11S):S20–6. [PubMed: 29055358]

[14]. Nelson JD, Shimazaki J, Benitez-del-Castillo JM, Craig JP, McCulley JP, Den S, Foulks GN. The international workshop on meibomian gland dysfunction: report of the definition and classification subcommittee. Invest Ophthalmol Vis Sci 2011;52 (4):1930–7. [PubMed: 21450914]

[15]. Knop E, Knop N, Millar T, Obata H, Sullivan DA. The international workshop on meibomian gland dysfunction: report of the subcommittee on anatomy, physiology, and pathophysiology of the meibomian gland. Invest Ophthalmol Vis Sci 2011;52(4):1938–78. [PubMed: 21450915]

[16]. Schaumberg DA, Nichols JJ, Papas EB, Tong L, Uchino M, Nichols KK. The international workshop on meibomian gland dysfunction: report of the subcommittee on the epidemiology of, and associated risk factors for, MGD. Invest Ophthalmol Vis Sci 2011;52(4):1994–2005. [PubMed: 21450917]

[17]. Sullivan BD, Evans JE, Dana MR, Sullivan DA. Influence of aging on the polar and neutral lipid profiles in human meibomian gland secretions. Arch Ophthalmol 2006;124(9):1286–92. [PubMed: 16966624]

[18]. Liu S, Hatton MP, Khandelwal P, Sullivan DA. Culture, immortalization, and characterization of human meibomian gland epithelial cells. Invest Ophthalmol Visual Sci 2010;51:3993–4005. [PubMed: 20335607]

[19]. Hampel U, Schröder A, Mitchell T, Brown S, Snikeris P, Garreis F, Kunnen C, Willcox M, Paulsen F. Serum-induced keratinization processes in an immortalized human meibomian gland epithelial cell line. PLoS One 2015;10:e0128096. [PubMed: 26042605]

[20]. Sullivan DA, Liu Y, Kam WR, Ding J, Green KM, Shaffer SA, Hatton MP, Liu S. Serum-induced differentiation of human meibomian gland epithelial cells. Invest Ophthalmol Vis Sci 2014;55(6):3866–77. [PubMed: 24867579]

[21]. Ziemanski JF, Wilson L, Barnes S, Nichols KK. Saturation of cholesteryl esters produced by human meibomian gland epithelial cells after treatment with rosiglitazone. Ocul Surf 2021;20:39–47. [PubMed: 33248214]

[22]. Phan MAT, Madigan MC, Stapleton F, Willcox M, Golebiowski B. Human meibomian gland epithelial cell culture models: current progress, challenges, and future directions. Ocul Surf 2022;23:96–113. [PubMed: 34843998]

[23]. Widjaja-Adhi MAK, Silvaroli JA, Chelstowska S, Trischman T, Bederman I, Sayegh R, Golczak M. Deficiency in Acyl-CoA:Wax Alcohol Acyltransferase 2 causes evaporative dry eye disease by abolishing biosynthesis of wax esters. Faseb J 2020;34:13792–808. [PubMed: 32851726]

[24]. Sawai M, Watanabe K, Tanaka K, Kinoshita W, Otsuka K, Miyamoto M, Sassa T, Kihara A. Diverse meibum lipids produced by Awat1 and Awat2 are important for stabilizing tear film and protecting the ocular surface. iScience 2021;24(5):102478. [PubMed: 34113821]

[25]. Rho CR, Kim SW, Lane S, Gao F, Kim J, Xie Y, Brown DJ, Skowronska-Krawczyk D, Jester JV. Expression of Acyl-CoA wax-alcohol acyltransferase 2 (AWAT2) by human and rabbit meibomian glands and meibocytes. Ocul Surf 2021;23:60–70. [PubMed: 34838721]

[26]. Baker BM, Chen CS. Deconstructing the third dimension – how 3D culture microenvironments alter cellular cues. J Cell Sci 2012;125:3015–24. [PubMed: 22797912]

[27]. Zouboulis CC, Yoshida GJ, Wu Y, Xia L, Schneider MR. Sebaceous gland: milestones of 30-year modelling research dedicated to the “brain of the skin”. Exp Dermatol 2020;29:1069–79. [PubMed: 32875660]

[28]. Asano N, Hampel U, Garreis F, Schroder A, Schicht M, Hammer CM, et al. Differentiation patterns of immortalized human meibomian gland epithelial cells in three-dimensional culture. Invest Ophthalmol Visual Sci 2018;59:1343–53. [PubMed: 29625457]

[29]. Benton G, Arnaoutova I, George J, Kleinman HK, Koblinski J. Matrigel: from discovery and ECM mimicry to assays and models for cancer research. Adv Drug Deliv Rev 2014;79–80:3–18.

[30]. Yoshida GJ, Saya H, Zouboulis CC. Three-dimensional culture of sebaceous gland cells revealing the role of prostaglandin E2-induced activation of canonical Wnt signaling. Biochem Biophys Res Commun 2013;438(4):640–6. [PubMed: 23948691]

[31]. Reneker LW, Wang L, Irlmeier RT, Huang AJW. Fibroblast growth factor receptor 2 (FGFR2) is required for meibomian gland homeostasis in the adult mouse. Invest Ophthalmol Vis Sci 2017;58(5):2638–46. [PubMed: 28510629]

[32]. Kim SW, Rho CR, Kim J, Xie Y, Prince RC, Mustafa K, Potma EO, Brown DJ. Jester JV. Eicosapentaenoic acid (EPA) activates PPARγ signaling leading to cell cycle exit, lipid accumulation, and autophagy in human meibomian gland epithelial cells (iHMGEC). Ocul Surf 2020;18(3):427–37. [PubMed: 32360782]

[33]. Kim SW, Xie Y, Nguyen PQ, Bui VT, Huynh K, Kang JS, Brown DJ, Jester JV. PPARγ regulates meibocyte differentiation and lipid synthesis of cultured human meibomian gland epithelial cells (iHMGEC). Ocul Surf 2018;16(4):463–9. [PubMed: 29990545]

[34]. Geueke A, Niemann C. Stem and progenitor cells in sebaceous gland development, homeostasis and pathologies. Exp Dermatol 2021;30:588–97. [PubMed: 33599012]

[35]. Xie HT, Sullivan DA, Chen D, Hatton MP, Kam WR, Liu Y. Biomarkers for progenitor and differentiated epithelial cells in the human meibomian gland. Stem Cell Transl Med 2018;7(12):887–92.

[36]. Kim SW, Brown DJ, Jester JV. Transcriptome analysis after PPARγ activation in human meibomian gland epithelial cells (iHMGEC). Ocul Surf 2019;17(4):809–16. [PubMed: 30742991]

[37]. Bickel PE, Tansey JT, Welte MA. PAT proteins, an ancient family of lipid droplet proteins that regulate cellular lipid stores. Biochim Biophys Acta 2009;1791:419–40. [PubMed: 19375517]

[38]. Hwang HS, Xie Y, Koudouna E, Na KS, Yoo YS, Yang SW, Brown DJ, Jester JV. Light transmission/absorption characteristics of the meibomian gland. Ocul Surf 2018;16(4):448–53. [PubMed: 30297027]

[39]. Parfitt GJ, Lewis PN, Young RD, Richardson A, Lyons JG, Di Girolamo N, Jester JV. Renewal of the holocrine meibomian glands by label-retaining, unipotent epithelial progenitors. Stem Cell Rep 2016;7(3):399–410.

[40]. Nicolas J, Magli S, Rabbachin L, Sampaolesi S, Nicotra F, Russo L. 3D extracellular matrix mimics: fundamental concepts and role of materials chemistry to influence stem cell fate. Biomacromolecules 2020;21(6):1968–94. [PubMed: 32227919]

[41]. Parfitt GJ, Brown DJ, Jester JV. Transcriptome analysis of aging mouse meibomian glands. Mol Vis 2016;22:518–27. [PubMed: 27279727]

[42]. Liu Y, Kam WR, Ding J, Sullivan DA. Effect of azithromycin on lipid accumulation in immortalized human meibomian gland epithelial cells. JAMA Ophthalmol 2014;132:226–8. [PubMed: 24357250]

[43]. Liu Y, Kam WR, Fernandes P, Sullivan DA. The effect of solithromycin, a cationic amphiphilic drug, on the proliferation and differentiation of human meibomian gland epithelial cells. Curr Eye Res 2018;43:683–8. [PubMed: 29283676]

[44]. Liu Y, Chen Di, Chen X, Kam WR, Hatton MP, Sullivan DA. Hypoxia: a breath of fresh air for the Meibomian gland. Ocul Surf 2019;17(2):310–7. [PubMed: 30528291]

[45]. Settembre C, Ballabio A. Lysosome: regulator of lipid degradation pathways. Trends Cell Biol 2014;24(12):743–50. [PubMed: 25061009]

[46]. Nien CJ, Massei S, Lin G, Liu H, Paugh JR, Liu C-Y, Kao WW-Y, Brown NJ, Jester JV. The development of meibomian glands in mice. Mol Vis 2010;16:1132–40. [PubMed: 20664693]

[47]. Parfitt GJ, Geyfman M, Xie Y, Jester JV. Characterization of quiescent epithelial cells in mouse meibomian glands and hair follicle/sebaceous glands by immunofluorescence tomography. J Invest Dermatol 2015;135:1175–7. [PubMed: 25398054]

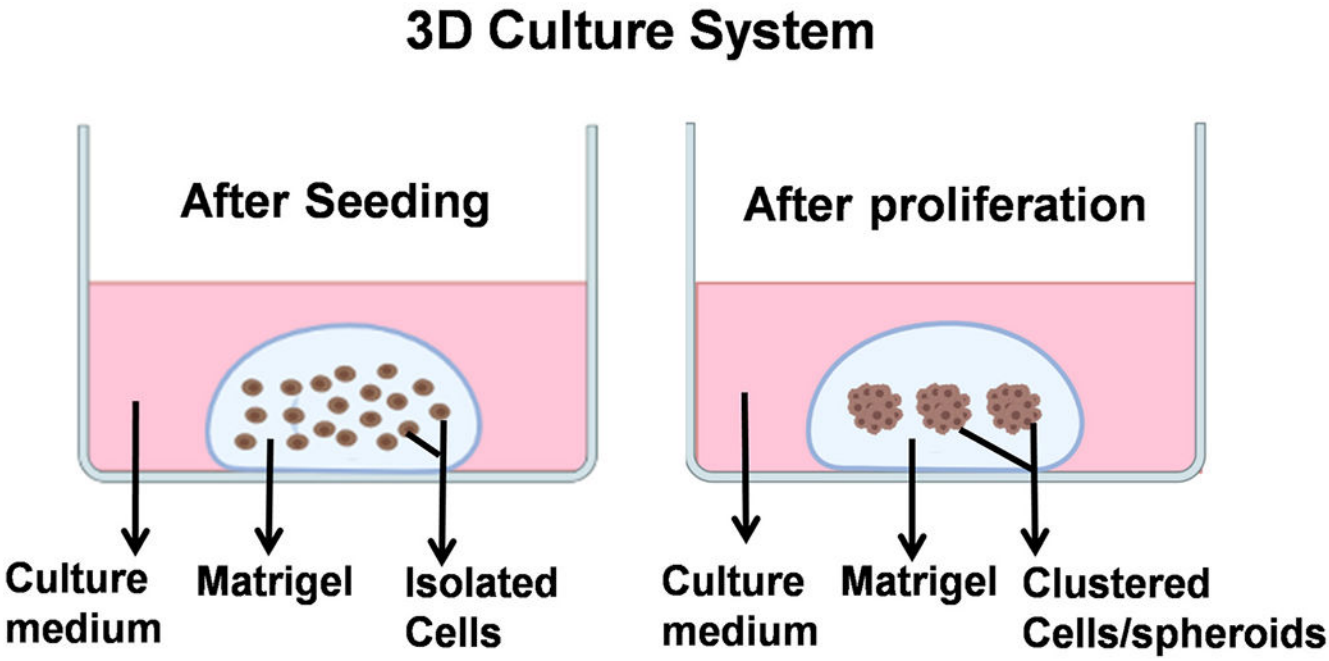

Fig. 1.
Diagrammatic illustration of 3D culture of iHMGEC in Matrigel® matrix.

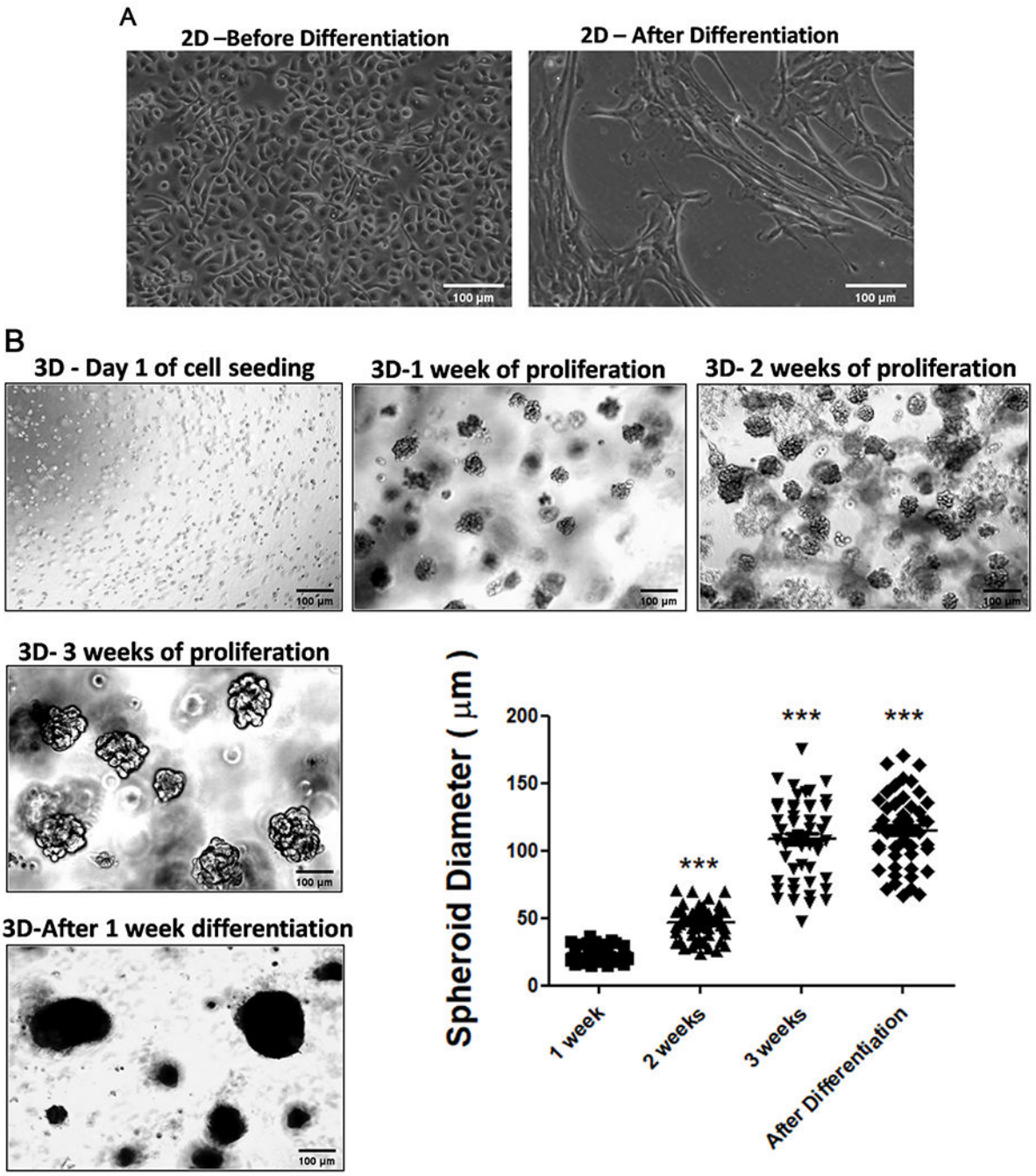

Fig. 2.

Generation of spheroids from iHMGEC. (A) 2D cell culture of iHMGEC; (B) Images showing iHMGEC spheroid formation at one week intervals during cell proliferation and clustering/spheroid formation and after differentiation, and a graphical representation of the average spheroid diameter. *** represents a P-value <0.001 compared to spheroid diameter at week 1). Spheroids sizes 23.5 µm ± 0.77 by 1 week, 46 µm ± 1.73 by 2 weeks, 121 µm ± 4.20 by 3 weeks, and 148 µm ± 3.73 after 1 week differentiation, Magnification is 10X.

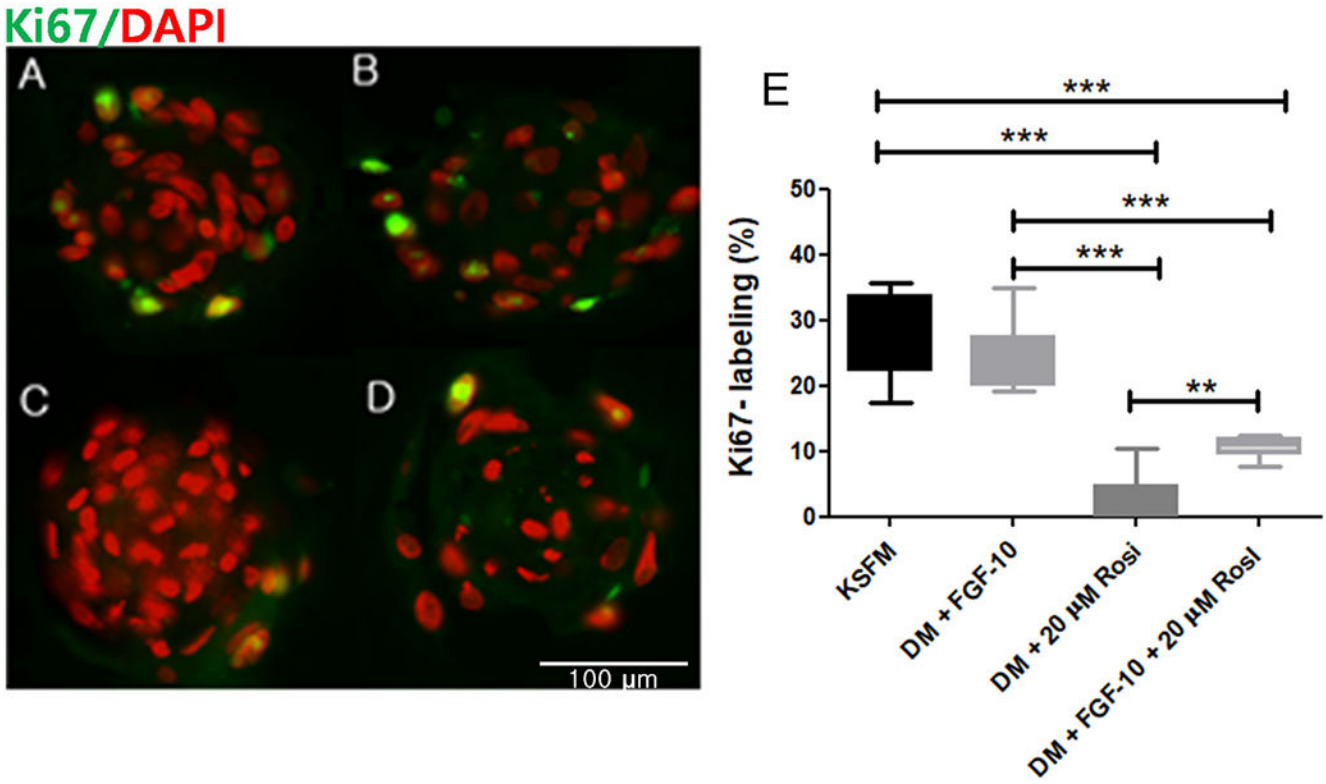

Fig. 3.

Expression of Ki-67 in 3D cultured iHMGEC spheroids

Representative IF images and their quantitative analyses for the expression of proliferation marker, Ki67, in spheroids cultured with KSFM (A), DMEM/F12 FGE10 (B), DMEM/F12 + rosiglitazone (C), DMEM/F12 + FGF10 + rosiglitazone (D). Quantitative analysis of the Ki67 labeling index is presented in E (*** represents P-value <0.001, ** represents a P-value <0.01, Green stain: Ki67; Red stain: DAPI. Magnification is 20X.

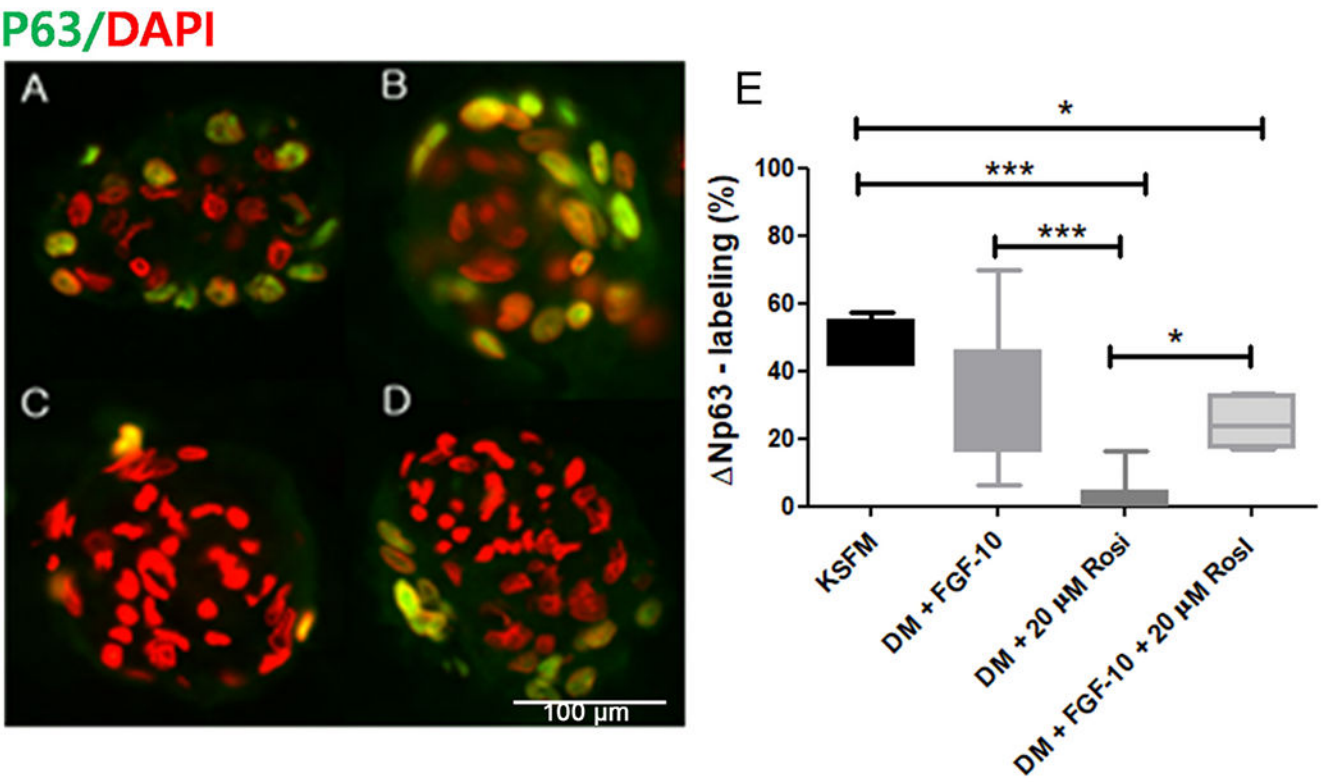

Fig. 4.

Expression of ΔNp63 in 3D cultured iHMGEC spheroids

Representative IF images and their quantitative analyses showing the expression of the epithelial progenitor cell marker, ΔNp63, in spheroids cultured in KSFM (A), DMEM/F12 + FGF10 (B), DMEM/F12 + rosiglitazone (C), DMEM/F12 + FGF10 + rosiglitazone (D). Quantitative analysis of the ΔNp63 labeling index is presented in E. (*** represents P-value <0.001, * represents P-value <0.05). Green stain: ΔNp63; Red stain: DAPI. Magnification is 20X.

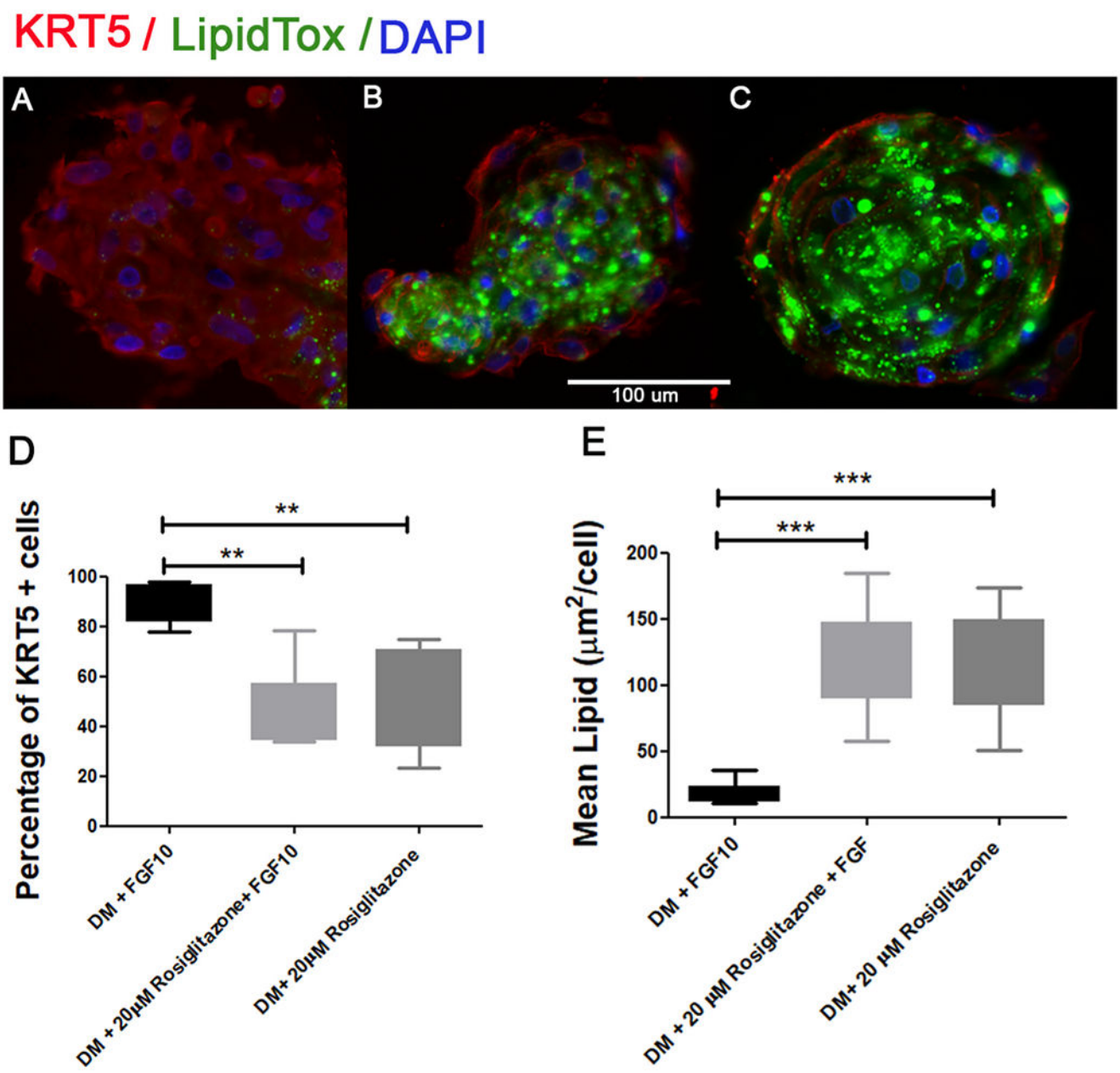

Fig. 5.

Expression of KRT5 and lipid droplet accumulation in the 3D cultured iHMGEC spheroids Representative IF images showing lipid droplets in spheroids co-stained with KRT5, cultured in DMEM/F12 + FGF10 (A), DMEM/F12 + rosiglitazone + FGF10 (B), and DMEM/F12 + rosiglitazone (C). Quantitative analysis is graphically presented for the expression of KRT5 (D) and lipid accumulation (E). (*** represents P-value <0.001, ** represents P-value <0.01). Red stain: KRT5; Green stain: Lipid; Blue stain: DAPI. Magnification is 20X.

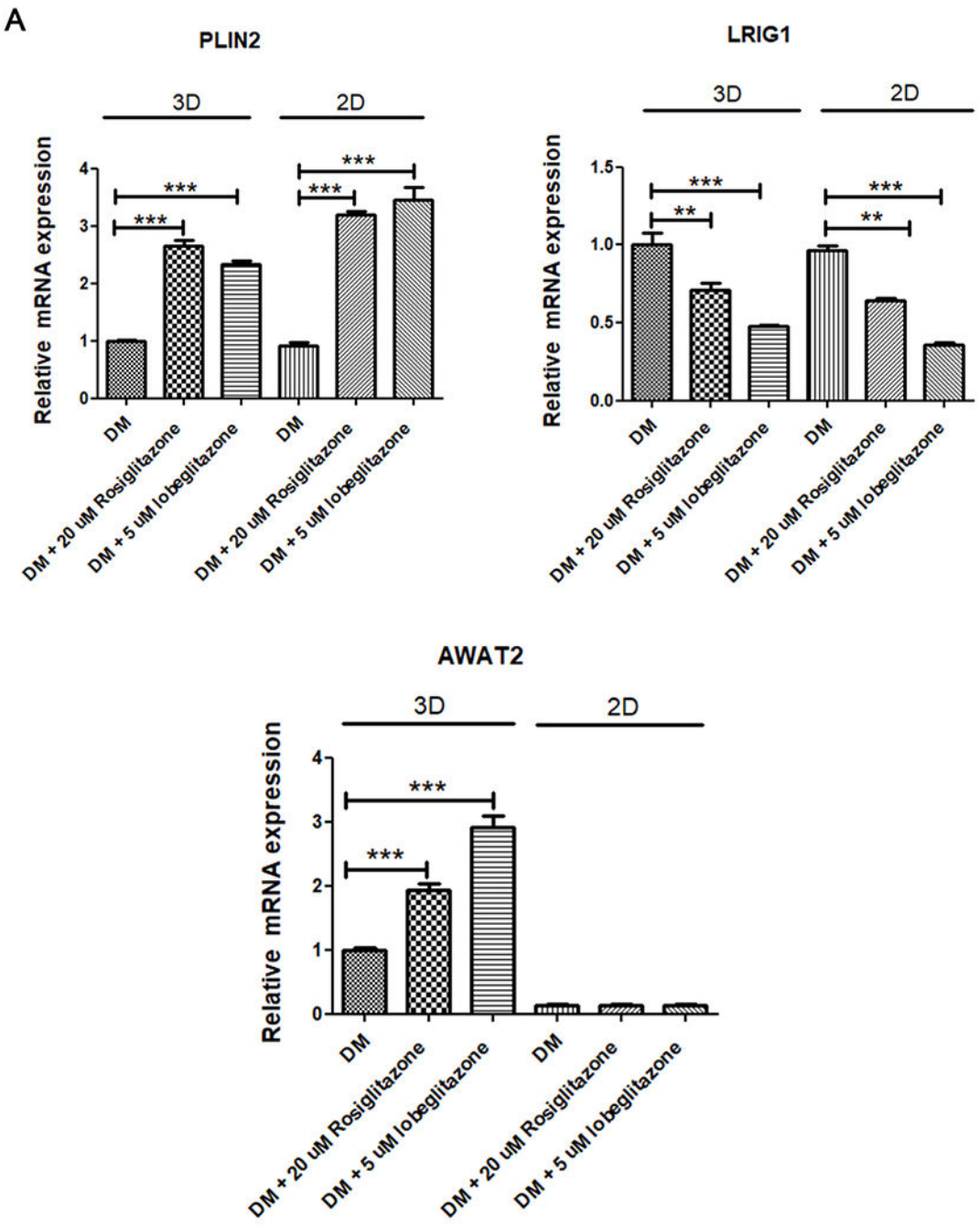

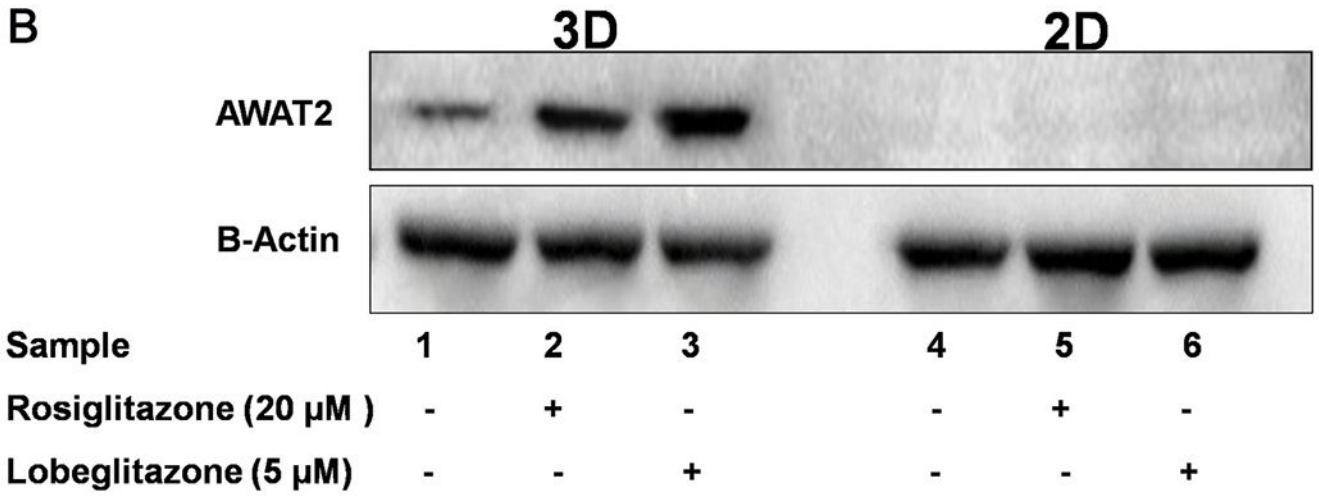

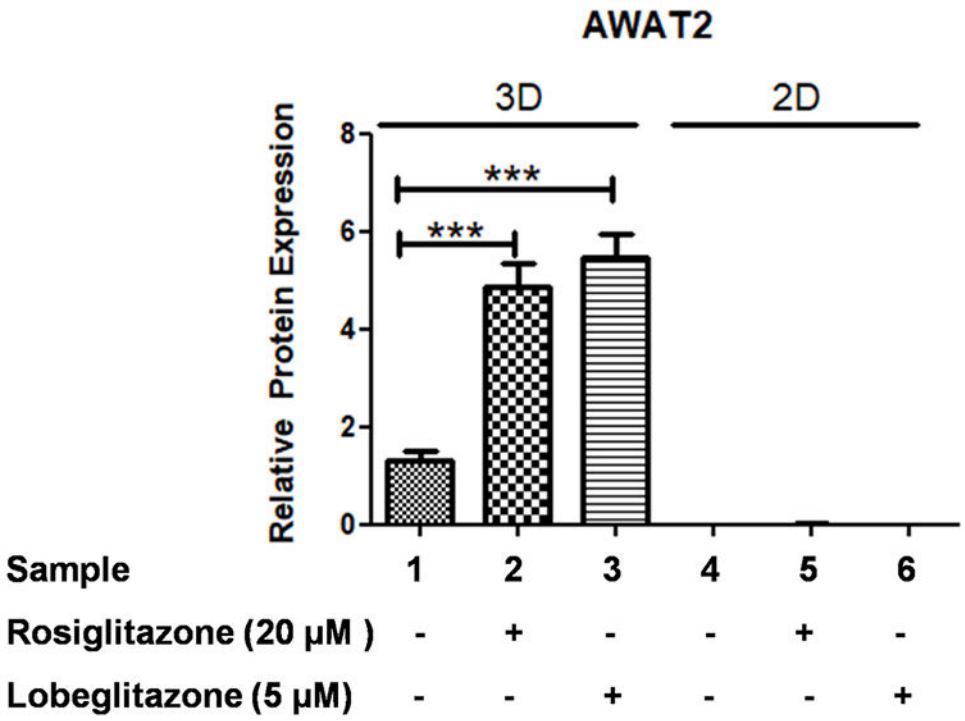

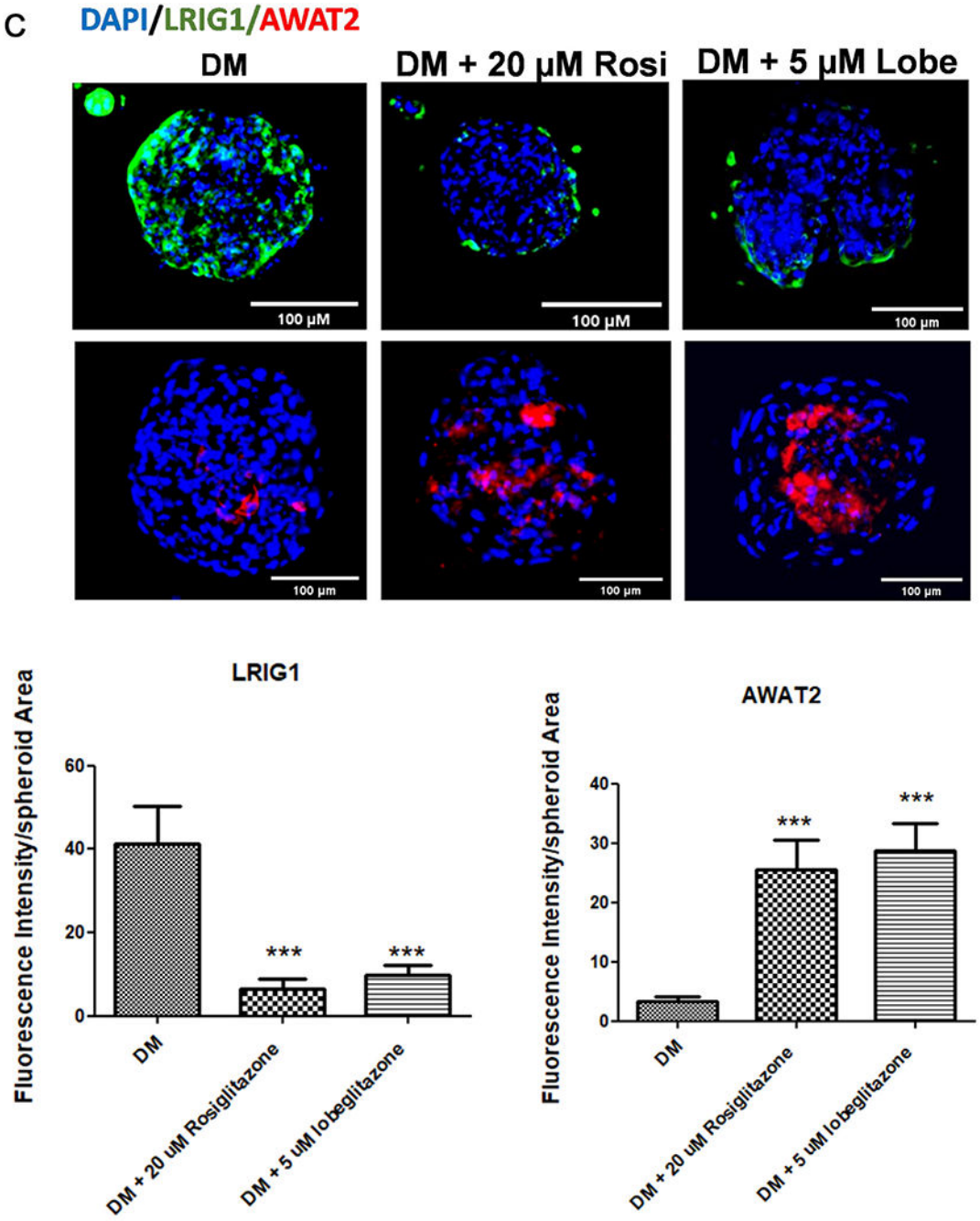

Fig. 6.

The 3D culture system promotes meibocytes differentiation and function. (A) Quantitative analyses of real-time PCR results showing the effect of PPARγ ligand treatment on PLIN2, AWAT2, and LRIG1 transcription in 2D and 3D culture systems; **(B)** Representative western blots and the quantitative analyses showing AWAT2 protein expression with PPARγ activation in 2D and 3D culture systems; **(C)** Representative IF images and the quantitative analyses showing AWAT2 and LRIG1 protein expression in spheroids (*** represents a

P-value <0.001, ** represents a P-value <0.01 compared with vehicle treated control). Green stain: LRIG1; Red stain: AWAT2; Blue stain: DAPI. DM:differentiation media.

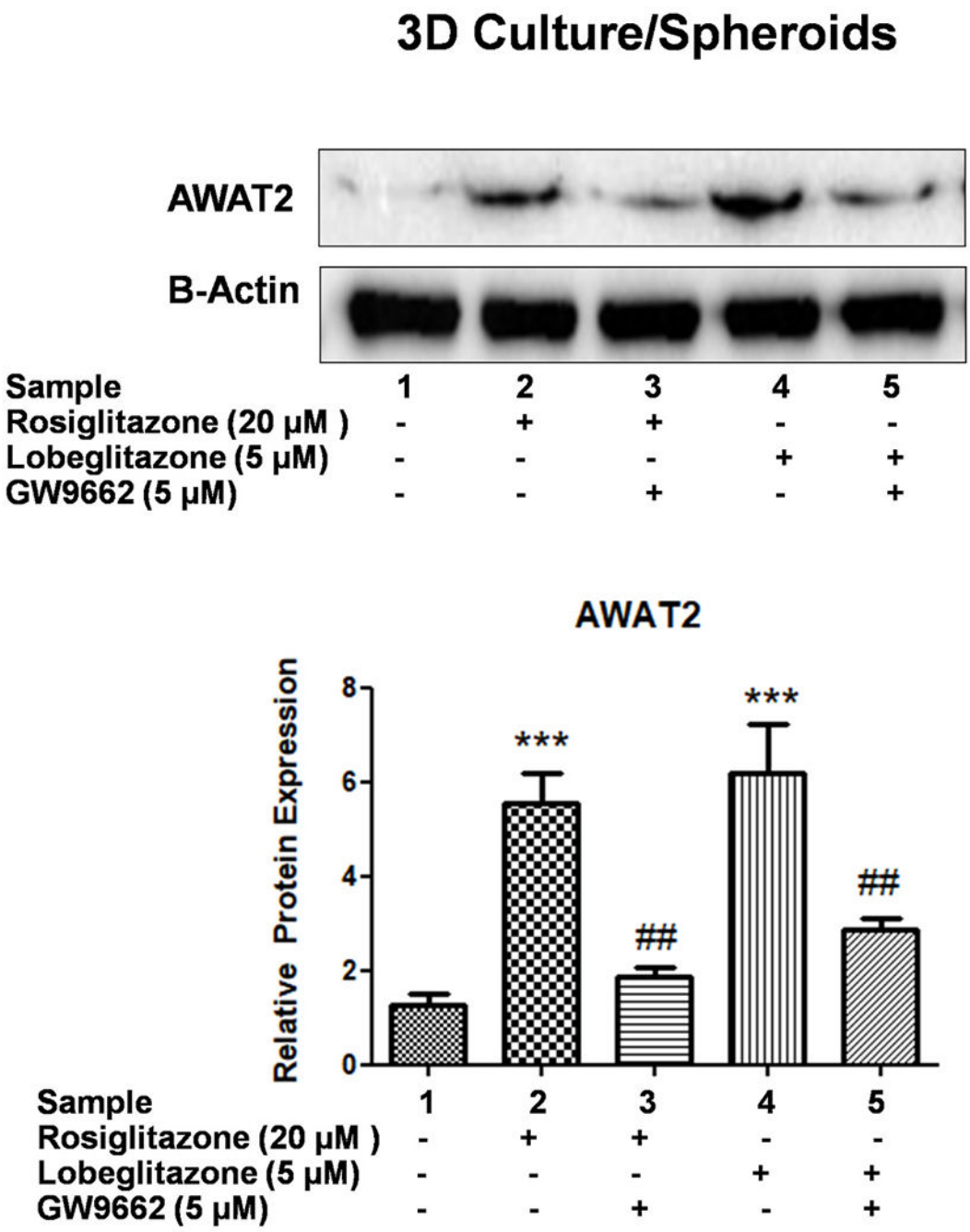

Fig. 7.

Modulation of AWAT2 syntheses by PPARγ signaling in 3D cultures. Representative western blots and the quantitative analyses showing AWAT2 protein expression with PPARγ ligand treatment with and without GW9662, a PPARγ inhibitor (*** represents a P-value <0.001 compared with the vehicle treated control, and ## represents a P-value <0.01 compared with the PPAR-γ ligands treated groups).

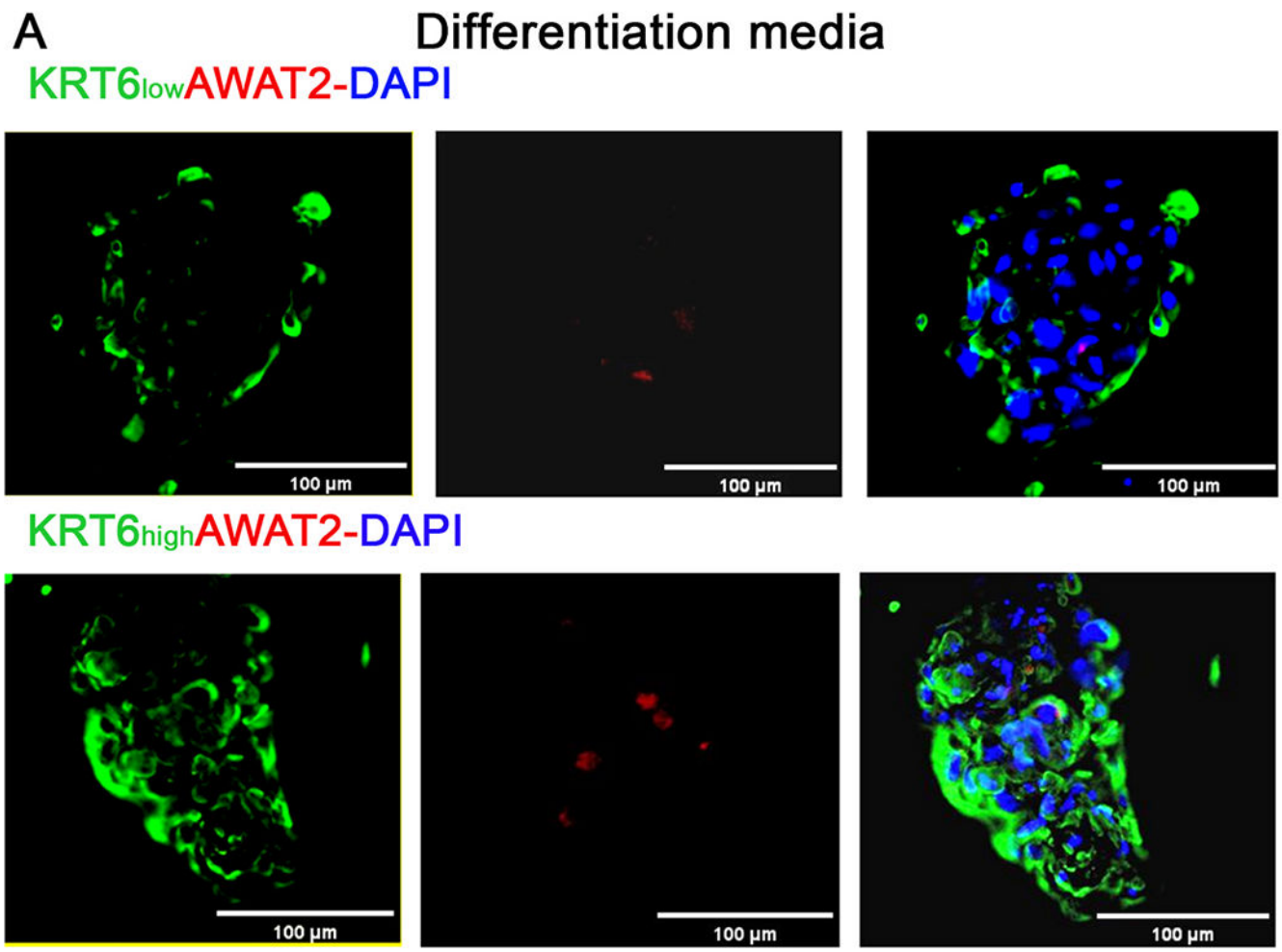

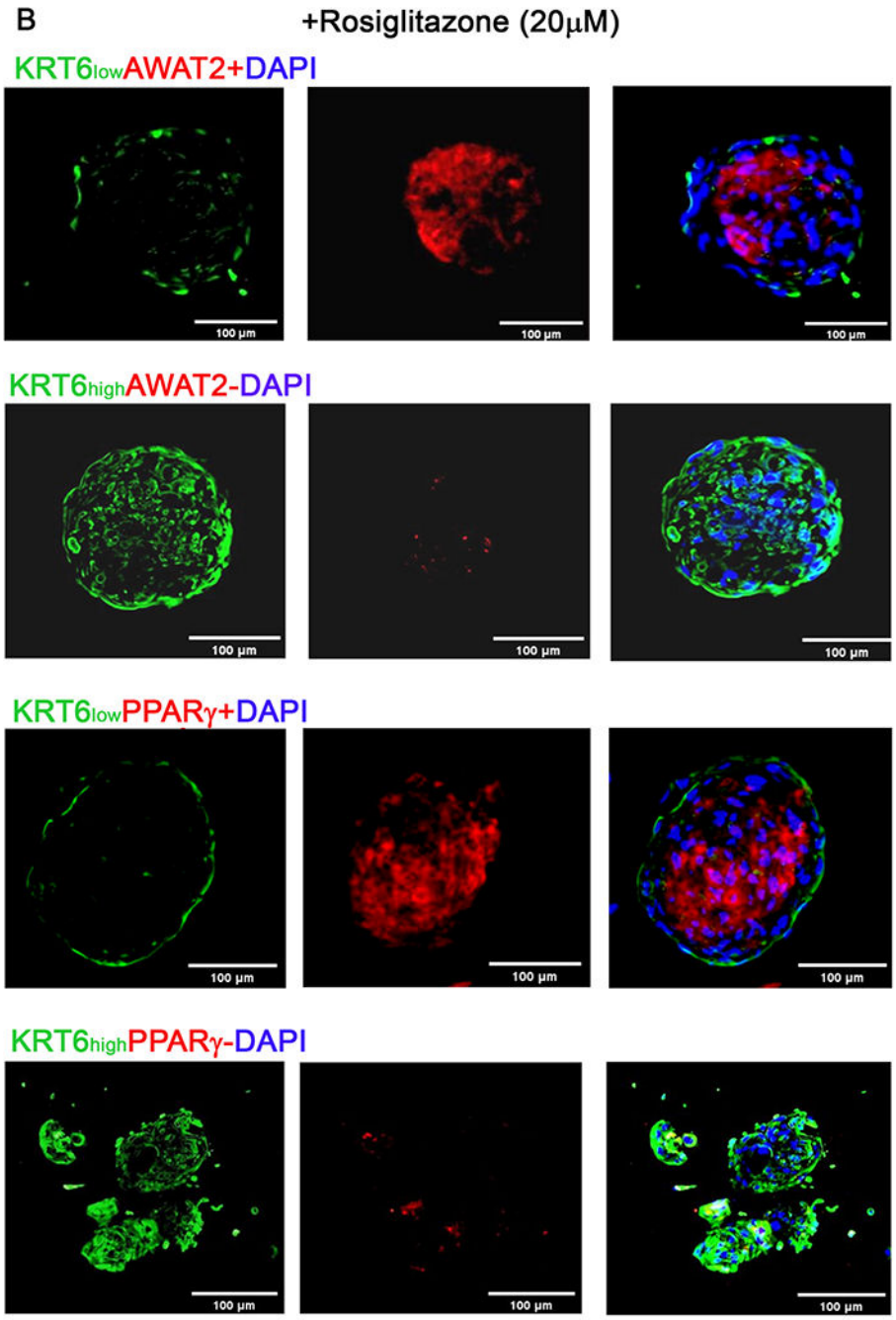

Fig. 8.

Immunofluorescence characterization of the iHMGEC in the spheroids. (A) Representative IF images showing KRT6/AWAT2 protein expression in spheroids cultured with DMEM/F12 alone (A) or in combination with rosiglitazone (B). Green stain: KRT6; Red stain: AWAT2/ PPAR-γ Blue stain: DAPI. Magnification is 20X, DM: differentiation media.